CFD Study for Downdraft Cooling in Large Buildings

J. S. Markus[1*], B. Bronsema[2*] and R. J. Schick
[1]Sprayings Systems Manufacturing Europe GmbH, Schorndorf, Germany
[2]Delft University of Technology, Netherlands
[3]Spraying Systems Co., Wheaton, IL 60187 USA

Abstract

Natural air conditioning with the Earth, Wind & Fire concept presents opportunities for multi-storey office buildings, hotels and apartment blocks. The core of the climate system is the Climate Cascade© which is designed as an architectural shaft and performs as a gravity-activated heat exchanger for conditioning the ventilation air. Ventilation air is being cooled or heated, dried or humidified as needed, by means of sprayed water droplets at the top of the shaft by full cone spray nozzles. The droplet size distribution applied here is not fine, as no cooling due to evaporation like for adiabatic cooling is required; instead the heat exchange is due to the inert heating of large amounts of cool, quite coarse water droplets of approximately 13 °C in summer and winter conditions. By momentum transfer from droplets to air, the downward air movement from the over pressure room is enhanced. This aerodynamic pressure, together with the hydraulic pressure and the downward thermal draft, reduces the need for fans. After successful testing in small scale the concept will be installed in a new hotel building in Amsterdam. This CFD study will explain the effect of the evaporation and condensation of a cool droplet spray computed with the Lagrangian discrete phase model. The model considered both evaporation and condensation at the same location and the computed temperature and relative humidity showed good agreement with the measured test results.

Keywords: Droplet evaporation, droplet condensation, discrete phase model, natural air conditioning

Introduction

The invention of air conditioning at the beginning of the last century and its subsequent further development has brought many benefits to society. Since the 1902 where Willis Carrier has tried to control humidity in a Brooklyn printing plant, using a fan-coil system similar like that previously installed the New York Stock Exchange air conditioning system, existing air conditioning improved and come common first in theaters and shopping centers. In 1919 the ASH&VE laboratory established the physiologically research of human comfort; comfortable indoor environments could significantly improve the well-being and productivity of people at their work. Soon factories and office buildings followed. In the 1950s air conditioning become Americas fastest growing industry, further encouraging air conditioning in U.S. government buildings. The influence of Victor Gruen's architecture of the weather protected closed box with indoor climate control and finally a wide spread growth also in private households, that was only shortly damped by the first world's energy crisis in 1979, enabled the fast growth of new productive cities even in the hot and humid regions. Today in the developed world we live in a place where nearly all large buildings are equipped with some heating ventilation air conditioning HVAC system.

Even though air conditioning is expensive and very energy inefficient, today we cannot imagine living without it, but nor do we really like it. Sometimes, it is even bad for our health. Many people are unsatisfied with the indoor climate at their workplace. There are many complaints about annoying fan noises, air quality, draughts and dry throats and eyes, which are notorious phenomena of the so-called sick building syndrome. Furthermore, the high energy use of air conditioning systems is increasingly becoming an issue, particularly in the light of the energy-neutral built environment that must become a reality in the near future.

But there is hope: a natural air conditioning concept is now ripe for large-scale application in existing and new buildings. Fan noise, draughts and dry throats and eyes will all become a thing of the past, and the air quality is just as good as outside. For energy use the most stringent European standard is easily exceeded by a factor of ten. As the American architect Richard Buckminster Fuller said: "You never change things by fighting the existing reality. To change something, build a new model that makes the existing model obsolete."

Natural Air Conditioning

Instead of shielding and eliminating contact with outside environment and the usage of lots of energy in climate-responsive architecture the weather and the natural resources like water, wind and sun are integrated. A conceptual cross section of a building with natural air conditioning is shown in figure 1. This building does not have an air handling system installed. Instead, the building itself functions as an air conditioning machine using the sun, wind and gravity. The design of a climate-responsive building requires close cooperation with the architect.

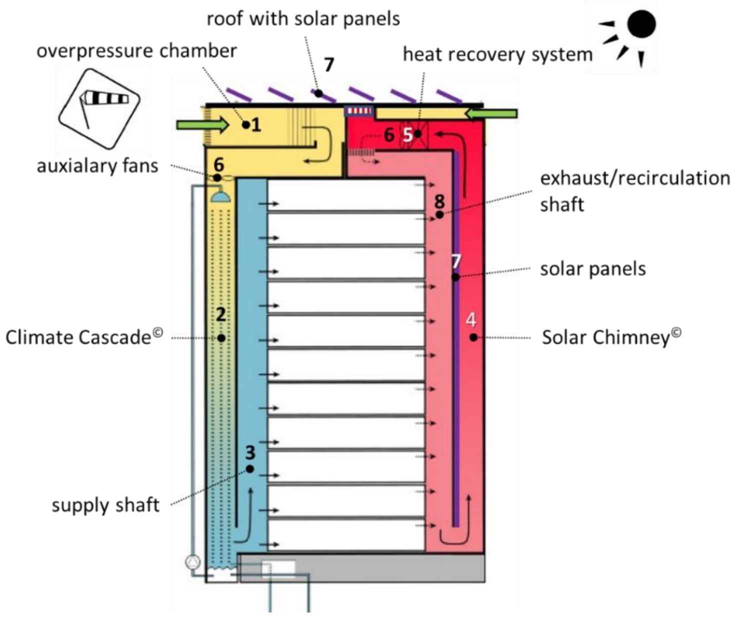

Figure 1 Principles Earth Wind & Fire natural air conditioning. (This figure illustrates the EW&F 2.0 concept. The original EW&F concept had a Venturi roof system for extracting air. An EW&F 3.0 concept with wind turbines on a convex roof is currently under study.)

Just as the air handling unit, the system is based on separate sections for air supply and extraction. Air supply is provided by the climate cascade (2), which is a structural shaft. Outside air flows into the building at the roof level and into the climate cascade by its way through the overpressure chamber (1). Cold water with temperature of 13 °C is sprayed at the top of the cascade, so that in summer the air is cooled to approximately down 7 - 8 °C. Cold is extracted from the ground using a TES system.

The large number of droplets in the spray together form a heat exchanger with a very large surface area, so that the system can generate tiny temperature differences between water and air. This heat exchanger has no air resistance, and in fact produces pressure. This is because the specific mass of the water-to- air mixture in the cascade is considerably larger than that of the outside air, so that pressure is built up at the base of the climate cascade, which is used to distribute air throughout the building by means of the vertical supply shaft (3). Due to the high level of contact between the spray spectrum and the air, various matter carried by the outside air – possibly including particulate matter – is absorbed by the water and so improves the air quality. In the summer, the air is dried somewhat due to condensation of water vapour on the cold-water droplets. In winter the air is automatically humidified. The spray water must of course be thoroughly cleaned and disinfected.

This '*silent air conditioning*' concept does not require fans, and hence also no silencers. The odour enhancing spray spectrum replaces odour-emitting air filters. Air humidification is inherent to the system. Finally, the energy use of the spray pump is only a fraction of that of the fans used in traditional air conditioning.

The ventilation air is extracted through the exhaust/recirculation shaft (8), which is connected to the base of the solar chimney (4), a structural shaft provided with insulating glass and installed on or in a south-facing wall. The air in the solar chimney is heated by solar radiation, and the resulting thermal draught functions as an extraction fan for the air.

A heat recovery system (5) at the top of the solar chimney recovers heat from the building and the sun. The heat is either used directly in the building or transported by the TES system to the ground to restore the thermal balance. During business hours, the used air is exhausted from the roof. The air is recirculated by the extraction shaft (8) to recover solar heat outside business hours, for example during the weekend.

Auxiliary fans (6) ensure that air circulation is maintained under all circumstances. The energy for the fans is supplied by solar panels on the roof and in the solar chimney (7).

The integration of the solar chimney, climate cascade and air distribution system in the structural design requires close cooperation with the architect, who will therefore play a key role as technical and artistic co-designer of the climate system. In principle, the intensive cooperation between the architect and the climate engineer should improve the quality of the building as a whole, while at the same time reducing the failure costs. We hope to provide tools for the design and engineering of these buildings in near future.

CFD Model for Droplet Evaporation and Condensation

For the computation of flow inside the climate cascade the general CFD software ANSYS Fluent is applied. As turbulence model the realizable k-ε model with default parameters is used, as it is known for good convergence for evaporation coolers and predicts flow separation points for bended flow more correct than the standard k-ε model. As the height of the building is large the effect on the static pressure of the flow field is included by gravity. The gravitational acceleration of 9.81 m/s²; the standard state is given as absolute pressure $p_n = 101325\ \mathrm{Pa}$ and temperature $T_n = 273.15\ \mathrm{K}\ (= 0\ °\mathrm{C}\ = 32\ °\mathrm{F})$.

The effect of the water droplets on the humid air is computed by the Lagrangian approach. It is assumed that the droplet spray is dilute; this means the volume percentage is low. Each droplet (or particle denoted as p) in the model is represented by a parcel of droplets. Each droplet parcel represents an arbitrary number of droplets (in reality) and contains a small part of the total mass flow rate and of the spray. Each droplet parcel is tracked in the flow domain by numerical integration of the equation of motion of spherical particles including gravity and drag.

For droplet temperatures T_p that are larger than the vaporization temperature T_{vap} and lower than the boiling temperature T_{bp} of the evaporating species i the droplets will evaporate

$$T_{vap} \geq T_p > T_{bp} \tag{1}$$

The heat and mass transfer during evaporation is driven by diffusion and convection. The evaporation rate of a droplet is mainly determined by the difference between the concentration, the molar density, on the droplet surface and the surrounding bulk gas mixture and the mass transfer coefficient.

$$N_i = k_c\left(c_{i,surface} - c_{i,bulk}\right) \tag{2}$$

where

$N_i =$ molar flux in (kmol/m² s)

$k_c =$ mass transfer coefficient in (m/s)

$c_{i,surface} = c_{i,s} = \frac{p_{sat,i}(T_p)}{R\,T_p} =$ molar concentration at the droplet surface in (kmol/m³)

$c_{i,bulk} = c_{i,\infty} = \frac{p_i}{R\,T_\infty} = \frac{x_i\,p}{R\,T_\infty}$ molar concentration at the droplet surface in (kmol/m³)

The partial pressure p_i of species i is determined by total pressure p at the cell, $p_i = x_i\,p$, and the mole fraction xi. The mole fraction x_i of the mixture can be calculated from the mass fraction y_i and molecular weight M_i

$$x_i = \frac{y_i/M_i}{\sum_i y_i/M_i} = \frac{y_i}{M_i} M_{bulk} \tag{3}$$

and the bulk molecular weight of the gas mixture

$$M_{bulk} = \left(\sum_{i=0}^{n-1} \frac{y_i}{M_i}\right)^{-1} \tag{4}$$

For the diffusion driven mass transfer the evaporation rate is

$$\frac{dm_p}{dt} = M_i\,A_p\,k_c(c_{i,s} - c_{i,bulk}) \tag{5}$$

For the diffusion and convective driven mass transfer the evaporation rate is

$$\frac{dm_p}{dt} = k_c A_p \rho \ln(1 + B_m)\,, B_m = \frac{y_{i,s} - y_{i,\infty}}{1 - y_{i,s}} \tag{6}$$

where $y_{i,s}$ vapor mass fraction and $y_{i,\infty}$ or $y_{i,bulk}$ is the vapor mass fraction in the bulk gas. For further reference please refer to [2, 3].

In our case the water vapor mass fraction $y_{H2O,\infty}$ in each cell is computed on the cell thread position, it's temperature for the given species index water. The humidity in each cell is derived by the ratio of the partial pressure of water vapor in the cells gas mixture to

$$R.H. = \frac{p_{H_2O}}{p_{sat,H_2O}(T)} = \frac{y_{H_2O}/M_{H_2O}}{\sum_i y_i/M_i} \frac{p}{p_{sat,H_2O}(T)} \tag{7}$$

The saturation pressure for water here is computed by the following approximate functions

$$f_1 = 0.01\,(T - 338.15) \tag{8}$$

$$f_2 = \left(\frac{a_0}{T} - 1.0\right)\left(a_1 + f_1\left(a_2 + f_1\left(a_3 + f_1\left(a_4 + f_1\left(a_5 + f_1\left(a_6 + f_1(a_7 - f_1\,a_8)\right)\right)\right)\right)\right)\right) \tag{9}$$

$$p_{sat,H_2O}(T) = 22.089\ 10^{-6}\ e^{\min(f_2,\ 0.35)} \tag{10}$$

with

$a_0 = 647.286$; $a_1 = -7.419242$; $a_2 = 0.29721$; $a_3 = -0.1155286$; $a_4 = 8.685635\ 10^{-3}$; $a_5 = 1.094098\ 10^{-3}$; $a_6 = -4.39993\ 10^{-3}$; $a_7 = 2.520658\ 10^{-3}$; $a_8 = 5.218684\ 10^{-4}$

The algorithm to solve evaporation and condensation at droplets simultaneously is described in the following; it is coded in C in a special user defined function (UDF) compiled and linked to Fluent's solver:

Call the DEFINE_DPM_HEAT_MASS macro [4] and for each particle thread get cell, where the particle is inside. The pointer *particle* points to a data structure (struct). Get particle mixture material and gas mixture material components. Set

$n =$ TP_N_COMPONENTS(*particle*) = number of particle components
$M_i =$ molecular weight in (kg/kmol)
$T_p =$ particle temperature in (K)
$m_p =$ P_MASS(*particle*) = particle parcel mass in (kg)
$\rho_p =$ P_RHO(*particle*) = particle parcel mass in (kg/m^3)
$d_p = (\frac{6}{\pi} m_p/\rho_p)^{1/3} =$ DPM_DIAM_FROM_VOL(m_p/ρ_p) = particle diameter in (m)
$A_p =$ DPM_AREA(*particle*) = particle parcel surface in (m^2)
$Pr = \frac{c_p\,\mu}{k} =$ Prandtl number of gas mixture
$\mu =$ viscosity at cell in ()
$c_p =$ heat capacity at cell in ()
$k =$ heat conductivity at cell ()
$Re_p =$ Reynolds number of particle
$Nu = 2.0 + 0.6\, Re_p^{1/2}\, Pr^{1/3} =$ Nusselt number
$htc = \frac{k}{D_p} Nu =$ heat transfer coefficient in ()
$\frac{dh}{dt} = \frac{1}{A_p} htc(T_{cell} - T_p)$ heat source term in (kJ/)

Add the source terms of the particle temperature and component masses.

$$\frac{dT}{dt} = \frac{dy[0]}{dt} = +\frac{1}{m_p\, c_p}\frac{dh}{dt} \text{ in (K/s)} \tag{11}$$

Subtract the energy source term for the gas phase enthalpy

$$\frac{dz \rightarrow energy}{dt} = -\frac{dh}{dt} \tag{12}$$

Compute relative humidity of the cell as shown in equation (8); the saturation pressure of water at the cell temperature is computed by the function (9), (10) and (11) respectively.

Sum up the terms for all species *i* of the gas mixture to compute the bulk molecular weight as in function (4).

Begin to loop over all species *i* from $i = 0$ while $i < n$. If *i* equal an evaporating or condensing species of the mixture, then get

$T_{vap,i} =$ vaporization temperature for the evaporating or condensing species *i*
$D_i(T) =$ binary diffusivity for evaporating or condensing species *i* at cell temperature
$Sc = \frac{\mu}{\rho\, D_i}$ Schmidt number of the gas mixture
$k_c = \frac{D_i}{D_p}(2.0 + 0.6\, Re_d^{1/2}\, Pr^{1/3}) =$ mass transfer coefficient in (m/s)
$c_{i,bulk} = \frac{Y_i\, M_{bulk}}{M_i}\frac{p}{R\,T} =$ bulk gas concentration of the evaporating or condensing species *i* from ideal gas law

Compute the vaporization or condensation rate for each species as given in equation (5).

$$\dot{m}_{p,i} = M_i\, A_p\, k_c(c_{i,s} - c_{i,bulk}) \tag{13}$$

By default, in ANSYS Fluent there is no vaporization below vaporization temperature and hence no condensation. If $T_p < T_{vap}$ or $\dot{m}_{p,i} < 0$, then the vaporization rate is set $\dot{m}_{p,i} = 0$. Instead in this case we limit the evaporation rate only, if the relative humidity is $rh \geq 1$ and $\dot{m}_{p,i} > 0$. Then the mass transfer is limited to $\dot{m}_{p,i} = 0$. This allows mass transfer for $dm_p/dt < 0$ to get negative for $c_{i,\infty} > c_{i,s}$ and hence condensing.

Finally, at the end of the loop for each component the evaporation or condensing rate is subtracted from the particle components mass source term

$$\frac{dm_{p,i}}{dt} = \frac{dy[1+i]}{dt} = -\dot{m}_{p,i} \tag{14}$$

For each component the evaporation or condensing rate is added to the gas phase species mass source term

$$\frac{dz \rightarrow species[i]}{dt} = +\dot{m}_{p,i} \tag{15}$$

Subtract the heat transfer source terms and add the gas enthalpy source term

$$\frac{dT}{dt} = \frac{dy[0]}{dt} = -\frac{h_{vap,i}}{m_p\, c_p}\,\dot{m}_{p,i} \tag{16}$$

$$\frac{dz \rightarrow energy}{dt} = +h_{gas,i}\,\dot{m}_{p,i} \tag{17}$$

where

$h_{vap,i} =$ vaporization enthalpy of vaporizing or condensing component in (m/s)
$h_{gas,i} =$ enthalpies of vaporizing gas phase species in (m/s)

End of loop over all species at $i = n$.

At the end of the call of the DEFINE_DPM_HEAT_MASS for each particle thread this routine was computed, and the added source terms are updated in the solver solving the momentum and energy equation of the flow field. As the source terms due to condensation can make the convergence behaviour of the solver more unstable, for good convergence the underrelaxation factors for the terms of discrete phase model DPM had to be lowered to much smaller values, than default values. Hence, for an accurate, finally converged solution more iterations are required. This increases the total computational time and effort compared to solving the case limited to only evaporation.

CFD Results for Small Scale Test Setup

Before scaling up the model results were tested and validated over a long term at a small-scale test setup in a laboratory by Peutz bv. For a test scale model humid air flows through duct of 6 m height and an inlet velocity of 0.5 m/s. The area of the free cross section is 1 m x 1 m = 1 m^2. Water droplet are injected at the top of the duct by full cone spray nozzles. The droplet size distribution applied here is not fine, as no cooling due to evaporation like for adiabatic cooling is required; instead the heat exchange due to the inert heating of large amounts of cool, quite coarse water droplets and the warm humid air during their flight through the duct is desired.

In this work only the case for the design summer conditions will be discussed in detail. Altogether three different nozzle configurations had been modelled: One Single FullJet ® Nozzles of the type 1-1/2HH-30250, 4 or 5 rectangular aligned FullJet ® Nozzles 3/4GG-3050 were applied. The nozzles droplet size statistics had been measured for various gauge pressures in our laboratory in Schorndorf, Germany. It could be shown, that more nozzles result in a *more uniform* and a finer spray distribution. The corresponding fitted Rosin-Rammler size distribution applied for the case shown here had a mean volume diameter of 1600 µm and spread parameter of 2.5. The maximum gas velocity reached by smaller capacity spray nozzles is only up to 6 - 7 m/s due to momentum exchange between the droplets and the gas. A small back flow region (small swirl) can be found at rim in the top half of spray cone; for five smaller spray nozzles the swirling motion is less than in case of one larger single spray nozzle. Therefore, also a small part of droplets is carried back upwards at the rim of the tower. The droplet concentration below the nozzle is high >> 1 kg/m$_3$ and decreases to 100 – 200 g/m^3 inside the duct. While the droplets concentration inside the tower is quite uniform a fraction of the droplets might hit the side wall as more nozzles are aligned closer to the side wall. The temperature decreases from 28°C to 18.3 °C at the outlet, see fig. 2. A high relative humidity of 98.2% is reached, see fig. 3.

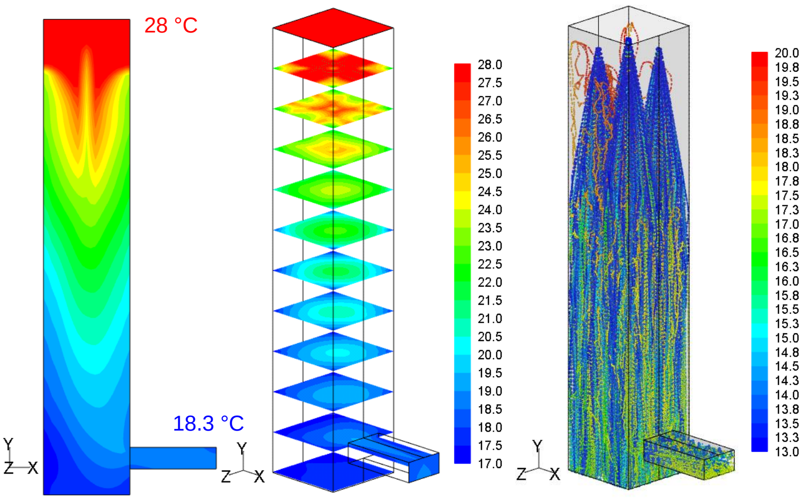

Figure 2 Humid air temperature (left) and droplet temperatures (right) in °C for small test setup at design summer conditions

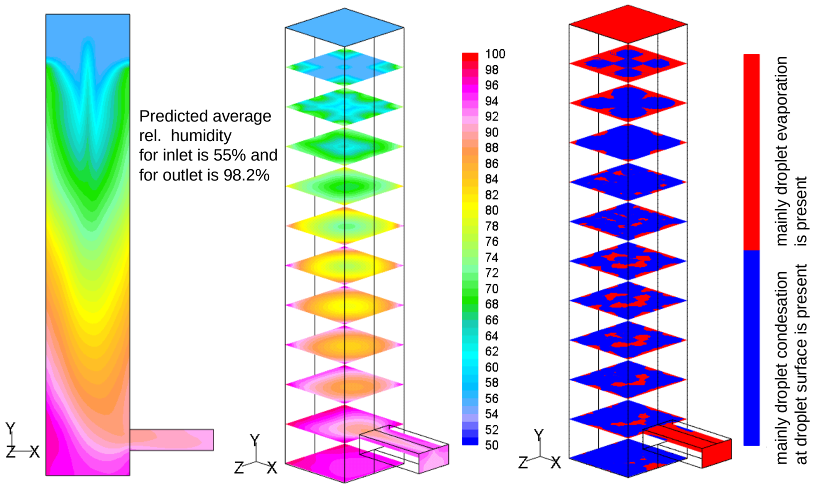

Figure 3 Relative humidity in % (left) and H_2O vapour mass source or sink (right) for small test setup at design sum

Mass transfer in the climate cascade

Figure 3 (right) shows also qualitatively the regions where droplet condensation or droplet evaporation dominates. Small droplets may grow slightly first and then shrink in diameter while temperature is rising above vaporization temperature along the path length. Small droplets are in the initial state so cold, that there will be back condensation at the droplet surface. In a hot environment the droplets are heated up. Due to this the continuous gas phase gets colder. The droplets temperature may increase further until even above the vaporization temperature. Now small droplets may evaporate, while large droplets, that are still below the vaporization temperature, are still heated up. For large droplets diameter is increasing slightly along the path length. At the end of the path length small droplets are heated more than large droplets. The droplet concentration below the nozzle is high >> 1 kg/m_3 and decreases to 100 – 200 g/m^3 inside the duct at the side wall.

The model was tested under different weather conditions. A comparison between the computed and measured operating conditions are listed in table 1. For the full modelling and test results please refer to Bronsema [1].

Table 1 Set, computed and measured operating conditions for the test setup

Weather Conditions	Design Summer		Average Summer		Cold Weather		Average Winter	
Humid Air								
Operating Pressure	101	kPa	101	kPa	101	kPa	101	kPa
Set Inlet Temperature	28	°C	20	°C	10	°C	5	°C
Measured Inlet Temperature	27.3	°C	20.0	°C	10.1	°C	5.3	°C
Set Rel. Humidity	55	%	80	%	90	%	90	%
Measure Rel. Humidity	51.9	%	77.7	%	100	%	95.3	%
Set Flow Rate	1800	m^3/h	1800	m^3/h	1800	m^3/h	1800	m^3/h
Measured Flow Rate	1789	m^3/h	1832	m^3/h	1836	m^3/h	1836	m^3/h
Computed Outlet Temp.	18.3	°C	15.8	°C	12.1	°C	8.8	°C
Measured Outlet Temp.	16.9	°C	15.2	°C	10.1	°C	5.3	°C
Computed Outlet R.H.	98.2	%	97.9	%	100	%	100	%
Measured Outlet R.H.	97.56	%	100	%	98.87	%	97.72	%
Sprayed Water								
Set Inlet Temperature	13	°C	13	°C	13	°C	13.0	°C
Measured Inlet Temp.	12.9	°C	13.0	°C	12.8	°C	13.1	°C
Set Flow Rate	2419	dm^3/h	2423	dm^3/h	2415	dm^3/h	2416	dm^3/h
Measured Flow Rate	2422	dm^3/h	2423	dm^3/h	2410	dm^3/h	2427	dm^3/h

Computed Average Temperature of Water Droplets	15.5 °C	14.4 °C	13.4 °C	10.8 °C
Measured Average Temperature of Water at Exit	15.1 °C	14.4 °C	12.1 °C	11.0 °C
Set Water / Air Mass Flow Ratio	1.17	1.17	1.01	1.08
Measured Water / Air Mass Flow Ratio	1.16	1.11	1.06	1.05

CFD Results for first Zero Energy Hotel Breeze

The Hotel BREEZE in Amsterdam IJburg Haveneiland-West will be the first building in the world with Earth, Wind & Fire natural air conditioning, fig. 8. The concept helps the building to achieve an EPC of -0.3. The concept has been adapted to the specific requirements that a hotel must deal with. For a comparison of parameters with those of traditional air conditioning please refer to [5, 6]. It is important to realise that a hotel has a higher specific energy use than an office building. The reasons for this is the relatively high pressure loss of the air distribution system due to the complex infrastructure and the requisite fire and constant flow valves for the hotel rooms. Therefore, auxiliary fans add to the total pressure as shown for the 3d case at design summer conditions in fig. 4. The humid air is cooled along the shaft length of the climate cascade as shown in fig. 5 right; while the relative humidity is increasing to 100%, fig. 5 right. The average facet temperature and relative humidity along the shaft length is shown fig. 6 left and the static pressure in fig. 6 right. A fraction of droplets hits the side walls and will not create a higher momentum on the air continuum.

It was also tested, if a simplified 2d model can predict similar results as the full 3d case. While for a simplified 2d case the mixing between the cold droplets and the hot humid air is overpredicted, for the 3d case the high bulk density of the spray cone is predicted more realistic and leads to a lower cooling rate near to the injection level. Pressure can only be predicted accurately for the 3d case. It is predicted that a small fraction of droplet, about 1.5% of the mass flow remains in the outgoing flow behind the water basin at the bottom chamber. It was suggested to design a swirling flow at the bottom of the climate cascade that may help to demist the outgoing flow from small remaining droplets.

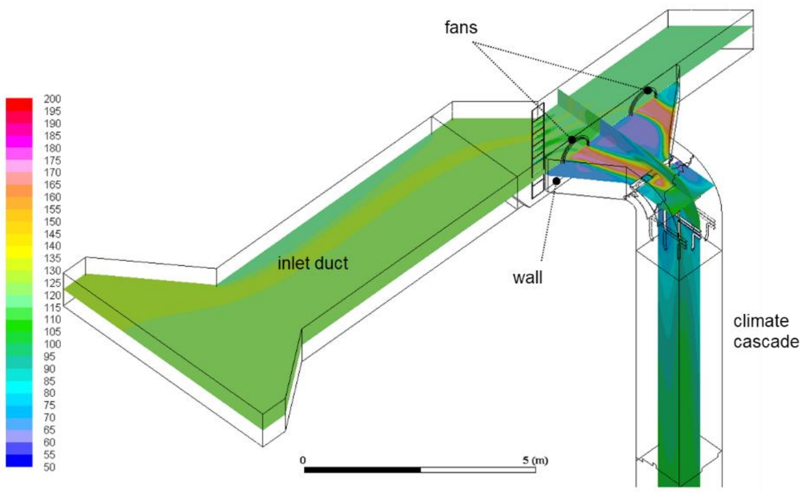

Figure 4 Total pressure in Pa with fans; directly behind the fans an additional pressure rise of +50 Pa is added

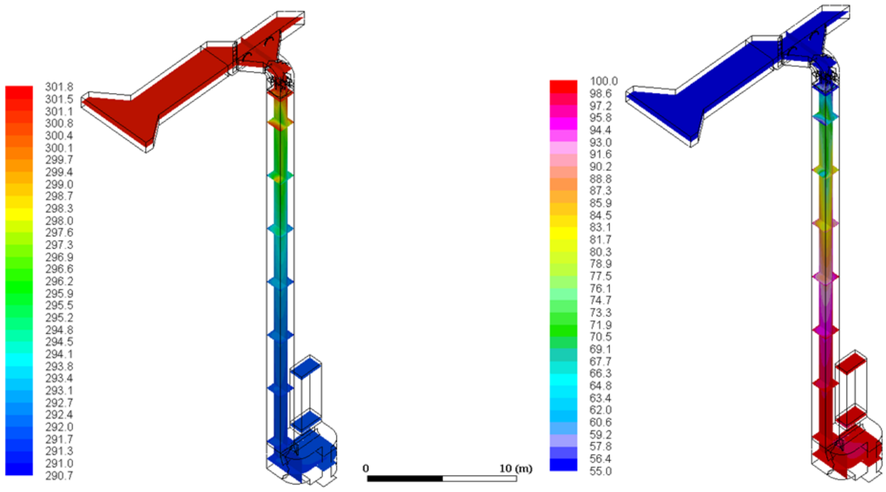

Figure 5 Temperature in K (left) and relative humidity in % (right)

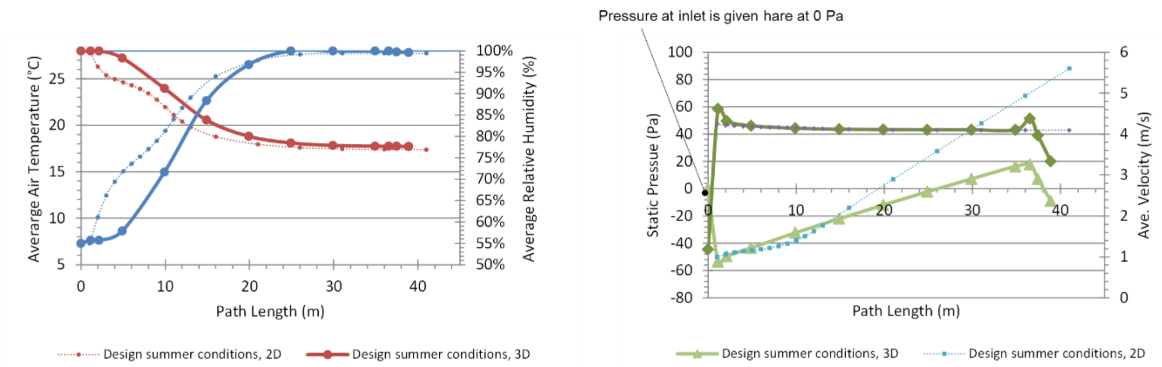

Figure 6 Design Summer Conditions Average Temperature and Relative Humidity over Height

The final computed results of the temperature and humidity ratio are plotted in the Mollier diagram for different operating and weather conditions in fig. 7. This shows clearly how the absolute water content of the incoming humid air for hot summer conditions is decreased while cooling, and how absolute water content of the incoming humid air for winter conditions is increased while heating inside the climate cascade.

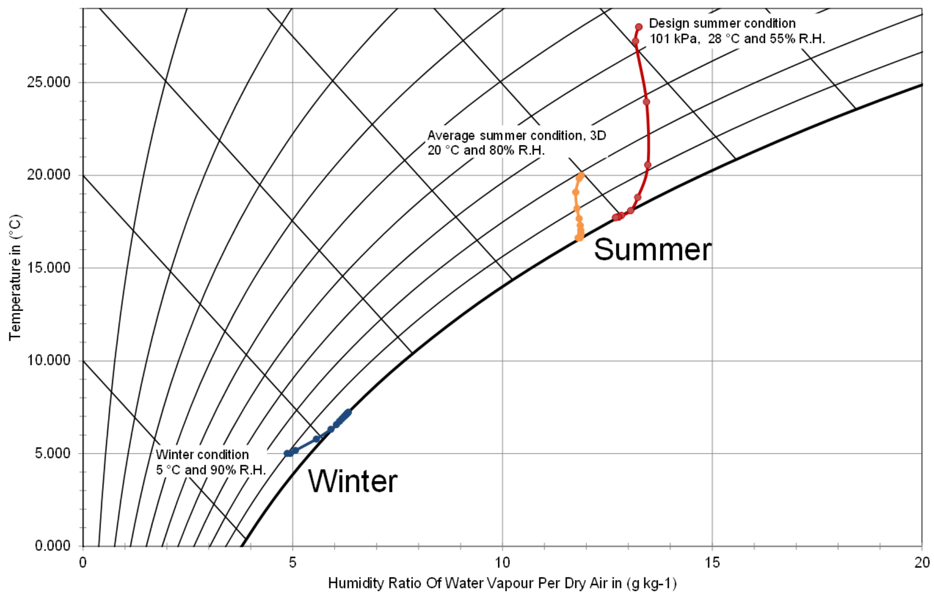

Figure 7 Mollier diagram for three different cases design summer, average summer and winter conditions

Figure 8 Actual project Breeze Hotel in Amsterdam IJburg; courtesy ECOncepts Hospitality / OZ Architecture / Dutch Green Company

Summary and Conclusions

The introduction of natural air conditioning can reduce energy use and improve the indoor environmental quality (IEQ). The Earth Wind & Fire concept was proven in test scale and is now applied to full scale for a new hotel building. As the installation of climate cascade requires equipment like pumps, piping spray nozzles, water treatment and control technology design engineers need tools to predict the pressure rise due to momentum exchange between the sprayed droplets and the humid air and the thermal conditions at the outlet of the Climate Cascade under various weather conditions. It could be proved that the Lagrangian *model including condensation and evaporation at the droplet surface* can predict and the total pressure rise and the thermal behaviour accurately. We hope that Earth Wind & Fire concept will have a positive impact for climate systems of office buildings, schools and other high residential buildings.

Acknowledgements

The Earth, Wind & Fire concept described above was developed as part of PhD research in a joint venture involving TU Delft, TU Eindhoven and external partners. This research demonstrated that the system is suitable for application in practice. The research was carried out with a grant from the Ministry of Economic Affairs, Agriculture and Innovation under the Energy Research Grants scheme: long term (Article 18b). Special thanks goes to Maarten Quist (director of Dutch Green Company), the developer of Hotel BREEZE and initiator of the first practical application of the EW&F concept in the construction industry. The author also likes to thank Ulrich Postl from ANSYS Fluent, Germany for his help getting the first stable CFD results.

References

[1] Bronsema, B., *Earth, Wind and Fire Naturlijke Airconditioning* 97-201 Uitgeverij Eburon 2013, ISBN 978 90 597 2762 5, https://repository.tudelft.nl
[2] Asano, K., *Mass Transfer From Fundamentals to Modern Industrial Applications*, Wiley-VCH, ISBN 3-527-31460-1
[3] ANSYS® Fluent, 18.1, *Fluent Theory Guide*, chapter 16.4.2 and 16.4.6, ANSYS, Inc.
[4] ANSYS® Fluent, 18.1, *Fluent Customization Manual*, chapter 2.5.5, ANSYS, Inc.
[5] Bronsema, B., van Luijk, R., Swier, P., Veerman, J., Verrmeer, J., *Natuurlijke Airconditioning – waar wachten we nog op?* TVVL Magazine 01 2018 NATUURLIJKE AIRCONDITIONING
[6] Bronsema, B., Bokel, R., Bruggema H., Quist, van der Spoel, W., Swier, P., Vermer, J., Veerman, J., *Natuur-lik* venttilatie en luchtbehandeling via klimaatcascaade TVVL Magazine 01 2018 KLIMATCASCADE
[7] Bronsema, B., Bokel, R., van der Spool, W., *Earth, Wind & Fire - Natural Air Conditioning*, Healthy Buildings Europe 2015 18-20 May 2015 Eindhoven, The Netherlands